

# Assessment of Egypt's Red Sea coastal sensitivity to climate change

Mohamed E. Hereher<sup>1</sup>

Received: 3 September 2014 / Accepted: 15 March 2015 / Published online: 24 March 2015  
© Springer-Verlag Berlin Heidelberg 2015

**Abstract** A coastal sensitivity index (CSI) was developed to assess the response of the Red Sea coast in Egypt to climate change in terms of sea level rise and global warming. Six different variables pertaining to the intrinsic characteristics of the coast that extends to 1200 km were utilized, notably: coastal geomorphology, coastal slope, width of the coastal plain, shoreline exposure, fauna/flora and land use. Data have been extracted, manipulated and presented using remote sensing and GIS analysis. The resulting coastal sensitivity map depicts the susceptibility levels of the Red Sea coastal plain to climate change. The most severely sensitive segments (very high CSI) account for 31 % (365 km) of the coast. They occur across unconsolidated, flat, wide, exposed, ecologically effective and/or inhabited coasts. On the other hand, the least sensitive (low CSI) coastal segments total 245 km (20 %) and are mainly rocky, steep, narrow, barren and/or inaccessible shores. Eustatic sea level rise by 1 m should inundate a coastal area of 106 km<sup>2</sup>, whereas a sudden tsunami of 5 m height should overwhelm 724 km<sup>2</sup>, particularly at the southern section near Shalateen. Global warming of seawater should impact the coastal zone between Hurghada and Marsa Alam (270 km long) due to the occurrence of fringing coral reef systems. The coastal sensitivity index provides a synoptic overview that could help prioritize emergency plans and protection strategies to reduce the ramifications of climate change.

**Keywords** Remote sensing · GIS · Coral reefs · Mangroves · Sea level rise · Global warming

## Introduction

The frequency, severity and intensity of climate-induced hazards are likely to increase worldwide (IPCC 2001) as the sea level rise imposes the greatest challenge facing most of coastal areas (Johnston et al. 2014). Sea level was fairly stable for the past 3000 years; however, during the 20th century, the sea level began rising at a global average rate of 1.7 mm/year (Williams 2013). The sea level is expected to continue rising even if the global climate stabilizes in the next few decades (Nicholls 2002). Global warming and consequent melting of ice in the main glaciers are the direct reasons for the sea level rise (Meehl et al. 2005). However, there are two other causes, including: (1) tectonic changes either by coastal subsidence/uplifting or by sediment compaction, and (2) eustatic changes either by loading/unloading of ice sheets or by changes in the ocean circulation and wind patterns (Arnott 2010). The projected climate change and sea level rise will alter the environmental conditions along most of the world's coastlines by coastal flooding and damaging property and coastal habitats as well as deteriorating groundwater quality of coastal aquifers (Hereher 2014; Uddameri et al. 2014). Specifically, coastal and marine ecosystems are vulnerable to degradation due to the change in either water temperature or water level. For example, water temperature is one of the determining factors for the existing of coral reef communities. Any excess of the water temperature could deteriorate the coral/algal symbiosis and lead to corals bleaching or even their mortality (McWilliams et al. 2005). Hughes et al. (2003) suggest that by 2040 all current coral

✉ Mohamed E. Hereher  
mhereher@yahoo.com

<sup>1</sup> Department of Environmental Sciences, Faculty of Science, Damietta University, New Damietta City, Egypt

reefs will disappear due to the global warming of the seawater. Increasing carbon dioxide (CO<sub>2</sub>) concentrations in the atmosphere are expected to lower the ocean water pH, which in turn could decrease coral calcification and formation (Kleypas et al. 1999). On the other hand, mangroves which are rich ecological systems occurring at the intertidal zone are sensitive to climate change because their location is intimately contingent to the sea level (IPCC 2001). Identifying shorelines susceptible to climate change is necessary for more effective coastal zone management (Abuodha and Woodroffe 2010).

There is a wide range of approaches for quantifying the coastal responses to climate change, which are different from the coastal changes caused by human activities, such as removing of coastal sand dunes and lagoons (Skilodimou et al. 2002). The coastal vulnerability index (CVI) is the most widely scheme used to enumerate the degree of shoreline susceptibility to sea level rise (Thieler and Hammar-Klose 1999). This index utilizes factors depicting the geologic setting of the coast, e.g., rock type, slope and erosion pattern, as well as the physical setting of the seawater in terms of wave height, tidal range and the amount of regional sea level rise. The CVI was applied in the United States (Thieler and Hammar-Klose 1999; Hammar-Klose et al. 2003; Pendleton et al. 2004, 2005; Boruff et al. 2005), India (Rao et al. 2008) and Egypt (Hereher 2015). Some studies modified the original CVI by incorporating specific characteristics of the coast into the original CVI, such as tsunami run-up (Kumar et al. 2010), hydrologic setting of the coastal area (Ozyurt and Ergin 2010), land subsidence (Doukakis 2005), population density (Duriyapong and Nakhapakorn 2011), touristic activities (Kunte et al. 2014) and ecosystems at the coastal plain (Hereher 2014).

The term “sensitivity” has been used in this study because it is the most suitable to denote the sympathy of the entire coastal zone since it describes the extent of the physical, geological as well as ecosystem and socio-economic aspects of the coast (Boruff et al. 2005). Regardless of the difference in terminology between the coastal vulnerability index (CVI) and the coastal sensitivity index (CSI), both indices pursue the same procedures. The primary challenge is to identify the variables that best describe the intrinsic behavior of the coastal zone and their response to climate change (Hereher 2014). The CSI includes a number of components describing the inherent characteristics of the coastal zone. The variables utilized for the risk assessment could, therefore, be customized according to the nature of the coast. For example the tidal range in high-tidal coasts is an important factor to be considered in the assessment of the vulnerability index. Traditional CVI of Thieler and Hammar-Klose (1999) was applied to coasts of high-tidal range, which is not the case

along the Red Sea. This parameter is, hence, not applicable in the present study. Coastal erosion patterns must be considered if the coast is experiencing instability, particularly at deltaic beaches (Hereher 2015). Coastal erosion has not been reported at the Red Sea coast, due to the absence of permanent fluvial systems and consequently it is not considered in the current impact assessment. On the other hand, delicate ecosystems, such as mangroves are crucial in any vulnerability assessment. Land use of the coastal zone is very important issue to be involved in the assessment process because there is a direct damage to property and infrastructure by the sea level rise.

The suggested CSI is estimated by obtaining the net value of the six variables. Mathematically, it is the square root of the product of all ranked variables divided by the number of these variables, as follows:

$$CSI = [(G \times S \times W \times E \times F \times U)/6]^{1/2} \quad (1)$$

where *G* is the coastal geomorphology; *S* is the coastal slope; *W* is the width of the coastal plain; *E* is the shoreline exposure; *F* is the fauna/flora and *U* is the land use. Each variable is ranked for all coastal segments in an ordinary scale between 1.0 and 4.0, where 1.0 refers to the least hazard and 4.0 implies the very high impact. The resultant number, which represents the severity level of the coast to climate change is ranked as low; moderate; high and very high. The limits between these classes are determined by the percentile analysis (Pendleton et al. 2004).

### The study area

The Red Sea, which separates the African Continent from the Arabian Peninsula, is a semi-closed water body connecting the Mediterranean Sea at the north with the Indian Ocean at the south. The Red Sea mainly occurs in six countries: Egypt, Sudan, Eritrea and Djibouti on the west coast, and Yemen and Saudi Arabia on the east coast. Depths of the Red Sea are either shallow along the reef shores (<50 m); deep at the continental shelf (500–1000 m) or very deep in the central trench (>1000 m) (Saad 2010). Maximum width of the Red Sea is 355 km in the southern half and its minimum width is 30–40 km at the Strait of Bab El-Mandab in the south. In Egypt, the Red Sea extends for about 1200 km from the city of Suez at the north (Lat. 30°N) to the Egypt/Sudan border at the south (Lat. 22°N). The average width of the Red Sea in Egypt is about 200 km. Tides in the Red Sea are semi-diurnal with very low tidal range and water currents follow a NNW–SSE direction throughout the year (Churchill et al. 2014). Maximum wave height is 1.3 m and the wave direction is toward south (Frihy et al. 2006). Water temperature ranges from 20 to 26 °C (Caragnano et al. 2009). At the latitude of 27°45'N, the Red Sea

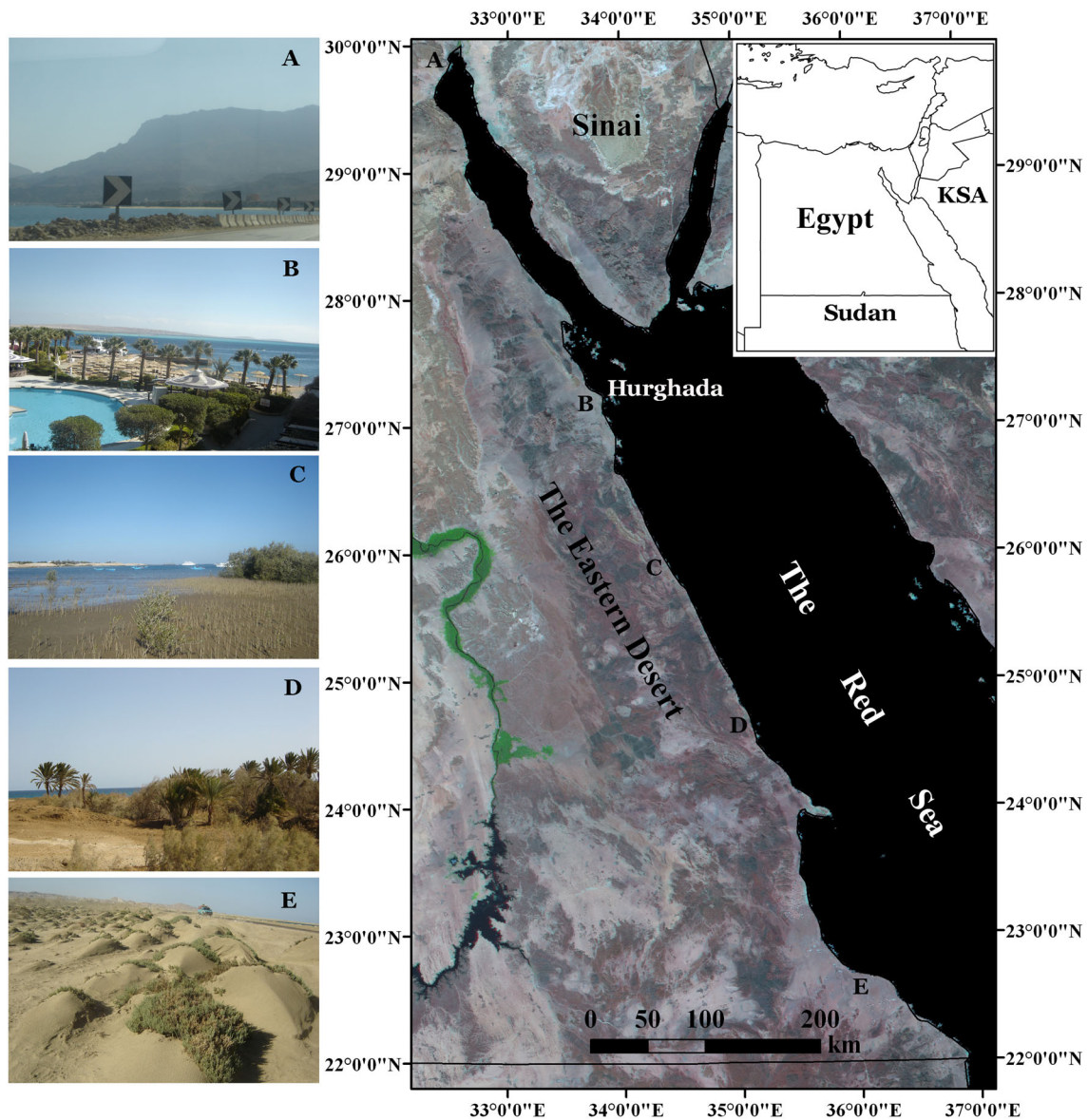


**Fig. 1** A MODIS image of the Red Sea revealing the physiography of the region. *Left* column represents some ground photos along the Red Sea coast. *Letters* from **a** to **e** are as following: **a** is the cliffy shore along the tip of the Gulf of Suez; **b** is a resort village at

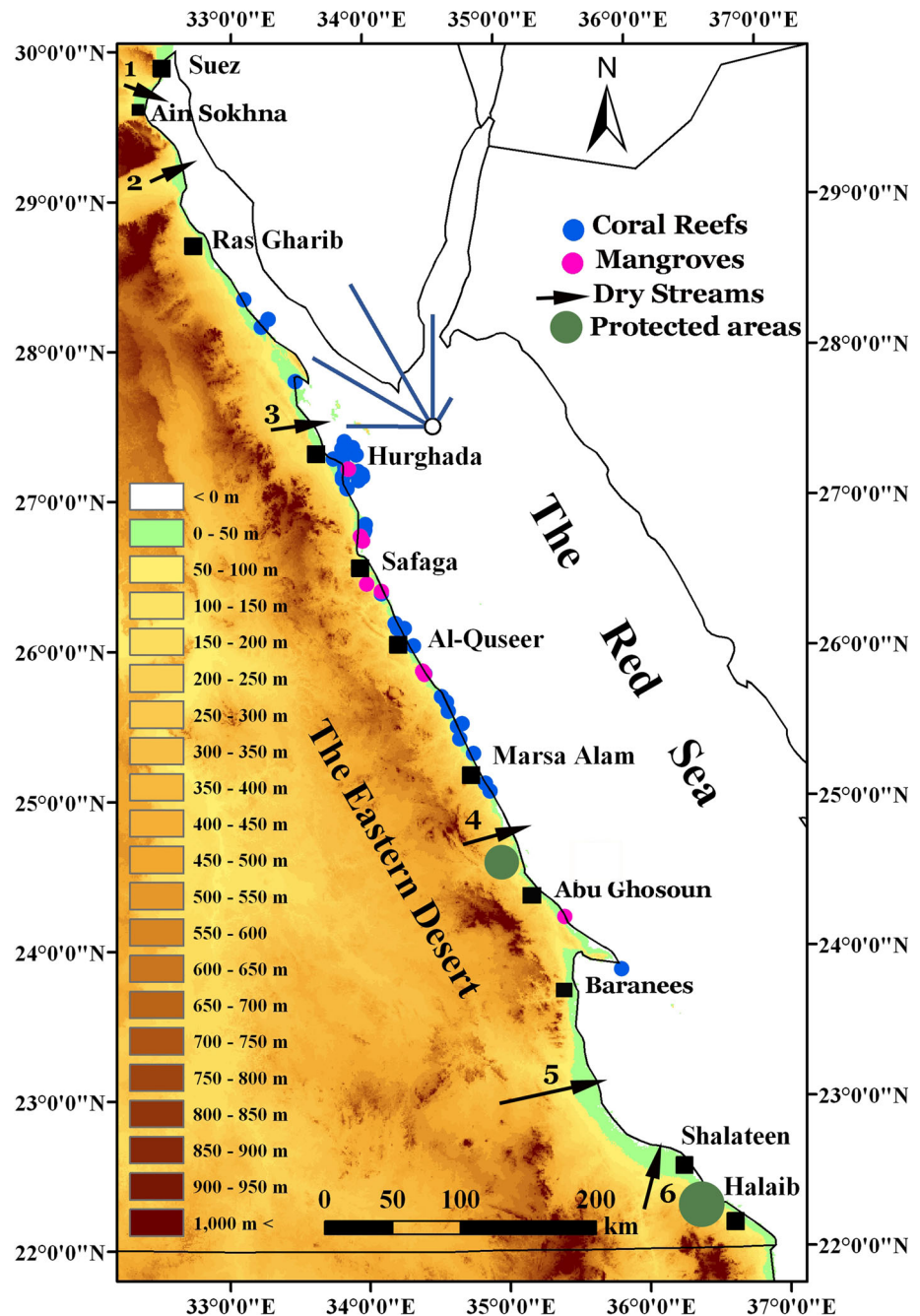
Hurghada showing the reef shore; **c** is a coastal lagoon at Safaga showing the mangrove vegetation; **d** is the coastal face of Wadi El-Gimal south of Marsa Alam; and **e** is the sandy beach at Shalateen

bifurcates to a V-shaped water body: the Gulf of Suez at the west and the Gulf of Aqaba at the east.

The Red Sea coast (Fig. 1) is referred to as a typical rift coast, where rifting began during the Oligocene and Miocene and has continued to evolve during the Pliocene (Plaziat et al. 1995). This coast is straight in a northwest–southeast direction for the most parts due to the tectonic origin of the Red Sea and is considered as a trailing edge coast (Davis 1996). The coastal plain is bordered from the west by very rugged mountainous series forming the structural edge of the Red Sea and representing the backbone of Egypt’s Eastern Desert (Said 1962). The sea side of

the coastal plain is bounded by fringing coral reefs (El Moursi et al. 1994). The width of the coastal plain varies from few meters along El-Galala Mountains at the Gulf of Suez to more than 35 km near Egypt/Sudan border. Raised coral reef terraces are frequent geomorphologic features widespread along the Red Sea coast, particularly between Hurghada and Marsa Alam. Mangrove vegetation occurs sporadically along the coastal flats and lagoons. There are numerous dry valleys draining the Eastern Desert highlands and terminating at the Red Sea (Fig. 2). The largest of these valleys are Wadi Araba along the Gulf of Suez, Wadi Hodein and Wadi Rahba near Shalateen in the south. Major

**Fig. 2** A digital elevation model showing the relief of the Red Sea coast and the adjacent Eastern Desert of Egypt. The rose diagram at Hurghada shows the direction of the prevailing wind. Locations of the coral reefs, mangroves and protected areas are shown in the map. Arrows refer to the main streams termination at the Red Sea, where 1 is Wadi Ghewebea; 2 is Wadi Araba; 3 is Wadi Abu Had; 4 is Wadi El-Gimal; 5 is Wadi Hodein and 6 is Wadi Shab



sediments and rock debris at the coastal plain were brought by these streams during torrential flashfloods that occurred in the Eastern Desert in the past. Coral reef assemblages are observed at the gaps between the mouths of the main dry streams. At some fans of these ephemeral streams some plant species, such as date palms (*Phoenix dactylifera*) grow naturally (Fig. 1) forming conspicuous diversified ecosystems. One of these valleys, Wadi El-Gimal (valley of camels) was declared as a protected area along the Red Sea. The Eastern Desert of Egypt, including the Red Sea coastal plain, is one of the least inhabitant regions of the

country. However, capital and private investments are the nation's most rapidly growing, particularly in the field of coastal tourism. Major settlement centers are Hurghada, Safaga, Al-Quseer, Marsa Alam, Baranees, Shalateen and Halaib. There are four main harbors at Suez, Ain Sokhna, Safaga and Abu Ghosoun. The geologic setting of the Red Sea coast has been reflected on the nature of the geo-environmental response to climate change that is completely different from the Mediterranean Sea coast, where coastal erosion is dominating, particularly along the Nile Delta promontories (Hereher 2014, 2015). The objectives of the

present study are to quantify and rank the relative response and sensitivity of the Egyptian Red Sea coastal plain to global climate change and projected sea level rise. Remote sensing and GIS analysis are the tools used to achieve the objectives of the study. These tools have been utilized effectively in the assessment of environmental management and geo-environmental hazards along coastal areas (Chaaban et al. 2012; Bathrellos et al. 2013; Youssef and Maerz 2013).

**Data and ranking of variables**

In order to develop a CSI for the Red Sea coast, the six variables suggested for the assessment (Eq. 1) were ranked on a linear scale from 1.0 to 4.0 for each variable, where 1.0 indicates that the variable has a low hazard level and 4.0 means that there is a very high threat upon the coast (Table 1). Coastal geomorphology was extracted from geologic maps of the Eastern Desert published by the Egyptian Geological Survey and Mining Authority (EGSMA). Satellite images from the Moderate Resolution Imaging Spectroradiometer (MODIS)—250 m spatial resolution acquired in 2014 were utilized to infer spectral information regarding the coastal plain and the shoreline orientation (exposure). Two MODIS images (h20v6 and h21v6) were mosaicked together and the appropriate bands were stacked in ERDAS Imagine for an on-screen visual interpretation of the coast. MODIS images were acquired from the NASA Land Processing Distributed Active Archive Center (LPDAAC). Wind data for Hurgada were provided by the Egyptian Meteorological Authority to determine the dominant wind direction as a surrogate for waves and currents direction. Digital elevation models (DEM) were acquired from the Shuttle Radar Topography Mission (SRTM) to determine both the coastal slope (in percent) and the width of the coastal plain. Seamless and finished 3 arc/sec (90 m spatial resolution) DEM data were acquired from the consortium of spatial information (CSI) for the tiles: 43/7 and 44/8. Fauna and flora of the study area refer to the coral reef assemblages and mangrove forests as well as brilliant plant communities occurring at the fans of the main wadis (valleys). The exact locations of

coral reefs were obtained from the database of the global distribution of coral reefs (Reefbase 2013). Sites of mangrove forests and vegetation communities were determined in the field using a hand-held GPS and were verified in fine resolution Google Earth images. Landsat-8 operational land imager (OLI)—30 m spatial resolution images acquired in 2014 were used to identify and interpret different land use of the coastal area. Settlements and other land use information were provided by the Central Agency for Public Mobilization and Statistics. Locations and information on the protected areas along the Red Sea coast were obtained from the Egyptian Environmental Affairs Agency (EEAA).

**Methods of the study**

**Coastal geomorphology**

Coastal geomorphology deals with the origin and development of landforms occurring along the coastline. It describes not only the rock type of the coastal area, but also the degree of resistance of such rocks to the wave action and the sea level rise. Cliffl shores have high resistance to waves and thus are low vulnerable, whereas unconsolidated deltaic sediments have the least resistance to wave action and, therefore, they are severely prone to inundation by the sea level rise (Rao et al. 2008). A rocky coast may include shores composed of materials ranging from hard rocks such as granite and basalt to relatively soft but cohesive materials (Finkl 2004). Rocky shores were identified by their tone in OLI images. Rocky shores are either cliffl, coral reef terraces or consolidated sedimentary strata. Cliffl shores were assigned a score of 1.0, meaning that the sensitivity to the sea level rise is low and reef shores were ranked as moderate with a value of 2.0. On the other hand, rocky limestone shorelines and fluvial terrestrial deposits were identified using geologic maps and were ranked as high vulnerable to sea level rise as they could dissolve by the prolonged erosion. These sedimentary strata were assigned a score of 3.0. The very high vulnerable coastal areas comprise friable sandy beaches, which could be

**Table 1** Limits and ranges of the variables utilized in the assessment of the CSI

Variable	Low (1)	Moderate (2)	High (3)	Very high (4)
Coastal geomorphology	Rocky–cliffl shores	Reef shores	Sedimentary (consolidated)	Sandy beaches
Coastal slope (%)	>18	12–18	6–12	<6
Width of the coastal plain (km)	<2.5	2.5–5.0	5.0–7.0	>7.5
Shoreline exposure	261°–350°	171°–260°	81°–170°	351°–80°
Fauna/flora	Rocky shores	Sedimentary shores	Fans of dry valleys	Corals and mangroves
Land use	Barren–abandoned–inaccessible	Protected areas	Industrial	Settlements resorts

identified by their light color (high albedo) in satellite images. They were verified in the field by the occurrence of sandy beaches and other sedimentary features, e.g., coastal dunes and sand heaps.

### Coastal slope

Coastal slope is the most important factor determining the response of coastal areas to flooding by seawater. Flat coasts are the most susceptible to sea level rise, whereas steep sloping coasts have the lowest vulnerability. Coastal slope was calculated in digital elevation models (DEM) using the slope tool of the “Spatial Analysis” in ArcGIS Software and the slope categories were carried out by pixel classification to yield four slope classes (Table 1). The slope was measured at the coastal strip extending for 10-km perpendicular to the shoreline. The least sensitive coastal regions are those with a coastal slope of more than 18 %. On the other hand, very high sensitive coasts are those which have gentle surfaces with coastal slopes less than 6 %.

### Width of the coastal plain

The width of the coastal plain determines the extent to which water could advance inland if the sea level rises slowly by global warming or accidentally by tsunami waves. If the coastal plain is narrow, the susceptibility to overwhelming should be low because water inundates limited inland area. On the other hand, if the coast has a wide backshore, then the inundation by the prolonged sea level rise or tsunami tides should be severe. In such a case, the harm and destruction to the coastal land use and the near-shore wildlife ecosystems are inevitable. It is therefore crucial to determine the areal extent of the coastal zone, which was proposed as the line occurring at 100 km distance from the coastline or at 50-m elevation; whichever is closer to the sea (Small and Nicholls 2003). In this study, DEM was used to determine the extent of the coastal plain. As the coast is generally narrow, the landward extent of the coastal zone was fixed at 50 m above the sea level using the “Buffer Zone” tool in ArcGIS Software package. The limits of the hazards concerning the width of the coastal plain were ranked between low (1.0) if the width of the coastal plain is less than 2.5 km and very high (4.0) if the coastal plain is wider than 7.5 km (Table 1).

### Shoreline exposure

This parameter relates the position of the shoreline to the direction of waves. If the shoreline is directly subjected to waves, the risk of inundation is much greater than the risk in sheltered shorelines. Wind data from Hurghada station

were analyzed and a wind rose was graphically prepared to determine the dominant annual wind direction as a proxy to the wave direction (Fig. 2). The orientation of the shoreline was measured in absolute degrees from the north direction (0–360°) and the degree of risk was determined in relation to the direction of the dominant wind direction, i.e., NW. Therefore shores directly facing the NW direction are the most vulnerable to the wave action. Shoreline exposure was classified into four categories (Table 1), as very highly exposed (351°–80°); highly exposed (81°–170°); moderately exposed (171°–260°) and low exposed (261°–350°) shorelines.

### Fauna/flora

Fauna and flora of the Red Sea are related to the occurrence of coral reef ecosystems, mangrove vegetation and other coastal plant communities existing at the fans of the alluvial systems (valleys) ceasing at the Red Sea. ArcGIS software was used to create point shapefiles of coral reef masses by their coordinates as provided by the database of the global distribution of coral reefs. Mangroves are generally confined to bays and lagoons, whereas important plant communities are contingent to dry streams, in which freshwater from floods sustains their survival. The occurrence of mangroves and plant communities was determined in the field and was verified in Google Earth images. Due to their very high sensitivity to global warming and sea level rise, coral reefs and mangroves were assigned a very high vulnerability class (4.0) (Table 1). Fans of dry streams are classified as highly sensitive regions (3.0) due to the harm that could exist to major plant communities. Sedimentary shores have been classified as moderately sensitive (2.0) as they may compose some *xeric* and *halophytic* vegetation communities. Rocky shores are generally void of significant vegetation communities and consequently were assigned a low sensitive class (1.0).

### Land use

Land use is an important socio-economic factor that is severely impacted by the sea level rise. Social and economic ramifications of global climate change should be considered because people would invest to construct their settlements. The direct impact of increased sea level, particularly sudden tsunami tides includes the loss of lives and property. Urban communities are usually under the threat of natural disasters if they occur either in repeated or high vulnerable areas (Bathrellos et al. 2012; Papadopoulou-Vrynioti et al. 2013). Therefore, coastal settlements and resort areas are very highly sensitive land use (4.0) (Table 1). Industrial land use refers mainly to the harbors occurring along the coast and it was considered as highly

sensitive (3.0) to sea level rise. Settlement and industrial locations were determined in satellite data, which is a well-documented approach (Al-Shalabi et al. 2013). Landsat-8 OLI images were the source of land use data in this study. Protected areas are important ecological systems occurring along the Red Sea coast. Although they are delicate and sensitive ecosystems, they were ranked as moderately sensitive (2.0) as they are extended into the adjacent desert. Barren unused coastal strips were considered the least impacted sectors as they have no land use. These abandoned shores were assigned as low sensitive (1.0).

**Coastal sensitivity index (CSI)**

The CSI was estimated for each point of the study area from the city of Suez at the north to the Egypt/Sudan border at the south as a net number produced by the six intrinsic variables of the coast as shown in Eq. (1). In order to manipulate the six variables instantaneously for each coastal point, a GIS analysis using the basic polyline functions in ArcGIS Software package was utilized. Each variable was produced as an individual map by digitizing the entire coastline to display the distribution of the four classes (1.0, 2.0, 3.0 or 4.0) for each point. The six generated maps were then overlain and each point, hence, has an attribute table with six values corresponding to the risk level. The resulted CSI for each coastal point was obtained from Eq. (1) using the simple vector algebraic technique. In order to determine the limits of the resulted CSI, a quartile classification was applied, where the discrete index values of the coastline were ranked according to their magnitudes. The lowest quarter (25th percentile) represents low CSI; 25th–50th percentile represents moderate CSI; 50th–75th percentile represents high CSI; and the highest

quarter (>75th percentile) represents very high CSI. Slicing the data by quartile analysis is consistent with the method applied by Thieler and Hammar-Klose (1999) for estimating the coastal vulnerability of the US coasts to sea level rise. A general coastal sensitivity map for the entire Red Sea coast of Egypt that extends for about 1200 km was then produced depicting the levels of coastal sensitivity to climate change. Although there is a little published information addressing the issue of the environmental sensitivity and coastal changes across the Red Sea coast, field observations and inspection were carried out at different sites in order to validate the accuracy of the CVI calculations.

**Results**

The maps of the six variables characterizing the intrinsic features of the Red Sea coast are shown in Fig. 3 and the magnitude (level) of each variable (low, moderate, high, and very high) for the entire coastal plain is shown in Fig. 4. The CSI map for the Red Sea coast is shown in Fig. 5 with the four sensitivity levels: low CSI; moderate CSI; high CSI and very high CSI. The calculated CSI ranges from 0.58 to 22.63 with a mean value of 7.84. The mode is 5.65; the median is 7.46 and the standard deviation is 5.35. The 25th percentile is 4.06; the 50th percentile is 7.46 and the 75th percentile is 11.31. CSI values below 4.06 are considered low; values ranging from 4.06 to 7.46 are considered moderate CSI; values ranging from 7.46 to 11.31 are high CSI and values greater than 11.31 are very high CSI. Lower CSI accounts for 20 % of the coast, moderate CSI represents 25 %; high CSI occurs at 24 % and very high CSI approaches 31 % of the entire coast

**Fig. 3** The distribution of the hazard level (from low to very high) of the six variables utilized in the present study

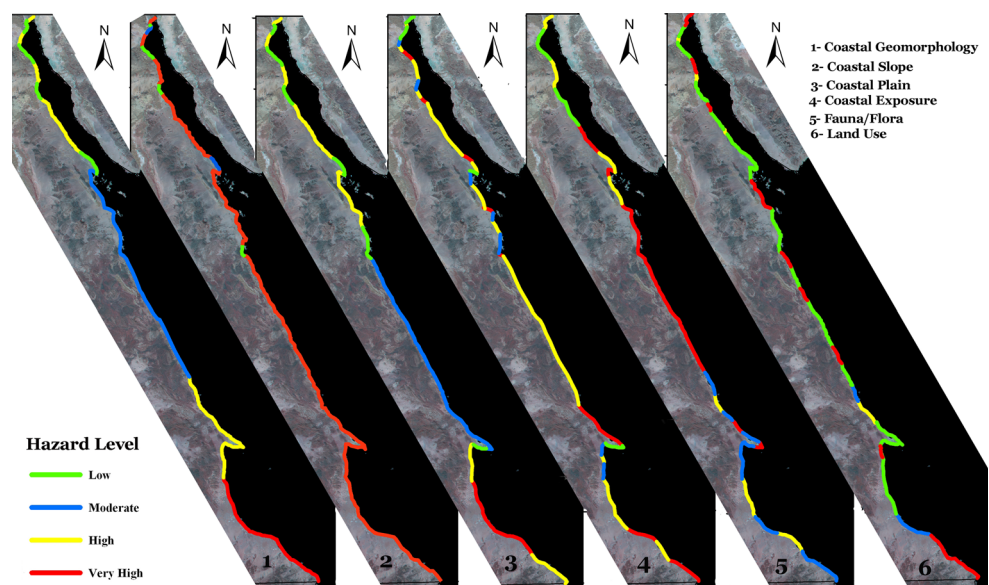


**Fig. 4** The magnitude of each hazard level of the six variables and the magnitude of the coastal sensitivity index

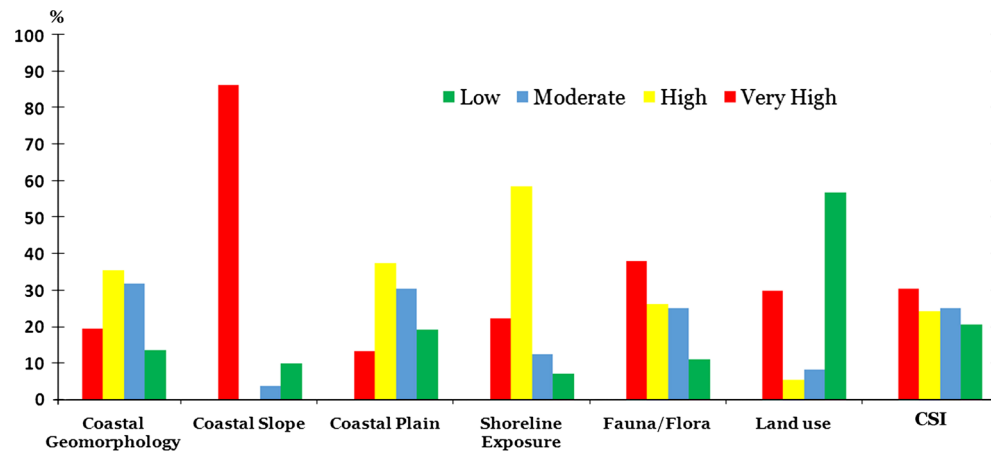


(Fig. 5). Minimum CSI (0.58) occurs at the foot of Ataq Mountain north of the Gulf of Suez, where the coastal plain is just a few meters. On the other hand maximum CVI is 22.63 for Shalateen in the extreme southern region which has an extended, gentle, and sandy beach.

### Coastal geomorphology

Coastal geomorphology reveals the occurrence of different coastal landforms. Cliffl shores of low risk to sea level rise extend for 13 % of the coast, mainly along the Gulf of Suez. They represent the coastal face of the main highlands in the region, e.g., the mountains of Ataq, El-Galala El-Baharaia, El-Galala El-Qiblia and Gebel Zeit. Moderate risk coasts comprise the reef shores predominating along the region between Hurghada and Marsa Alam. They occur either as offshore fringing systems or as raised terraces above the current sea level. Reef systems represent 32 % of the total coast. Although the backshore of the Red Sea coast is flanked by rugged terrain from the west, the coastline itself varies in depositional environments. The pediment plain in the west is a significant source of sediments that were transported from the rocky outcrops and then deposited during the Miocene until the Pleistocene by fluvial systems forming sedimentary strata (Said 1962). Other sedimentary shores are composed of limestone rocks, particularly at Ras Banas Peninsula (Abu Al-Izz 1971). The sedimentary shores account for 35 % of the coast and were ranked as high risk segments. The unconsolidated sandy beaches in the south represent 20 % of the coast and their mineral composition reveals their acidic-rock origin from the neighboring igneous rocks (Hereher and El-Ezaby 2012). They were brought to the coast by the biggest valleys in the region, i.e., Wadi Hodein and Wadi Rahba and they were ranked as very high risk coasts. Coastal sand dunes are observed along these sandy beaches.

### Coastal slope

Although the Red Sea is bordered by very rugged mountainous terrain from the west, the coastline is generally flat with a gentle slope for the majority (86 %) of its length. The Red Sea coastal area is, therefore, vulnerable to inundation by the sea level rise and it has a very high rank of sensitivity. On the other hand, steep sloping cliffs with low vulnerability to sea level rise represent only about 10 % of the coast and these shores occur along the Gulf of Suez in front of El-Galala El-Baharaia and El-Galala El-Qiblia Mountains. Moderate sloping coasts occur mainly at the coastal face of Gebel Zeit north of Hurghada and Ataq Mountain at the north of the Gulf of Suez, totaling 4 % of the study area. Coastal slope of 6–12 %, which is ranked as of high hazard, was not recorded in the region.

### Width of the coastal plain

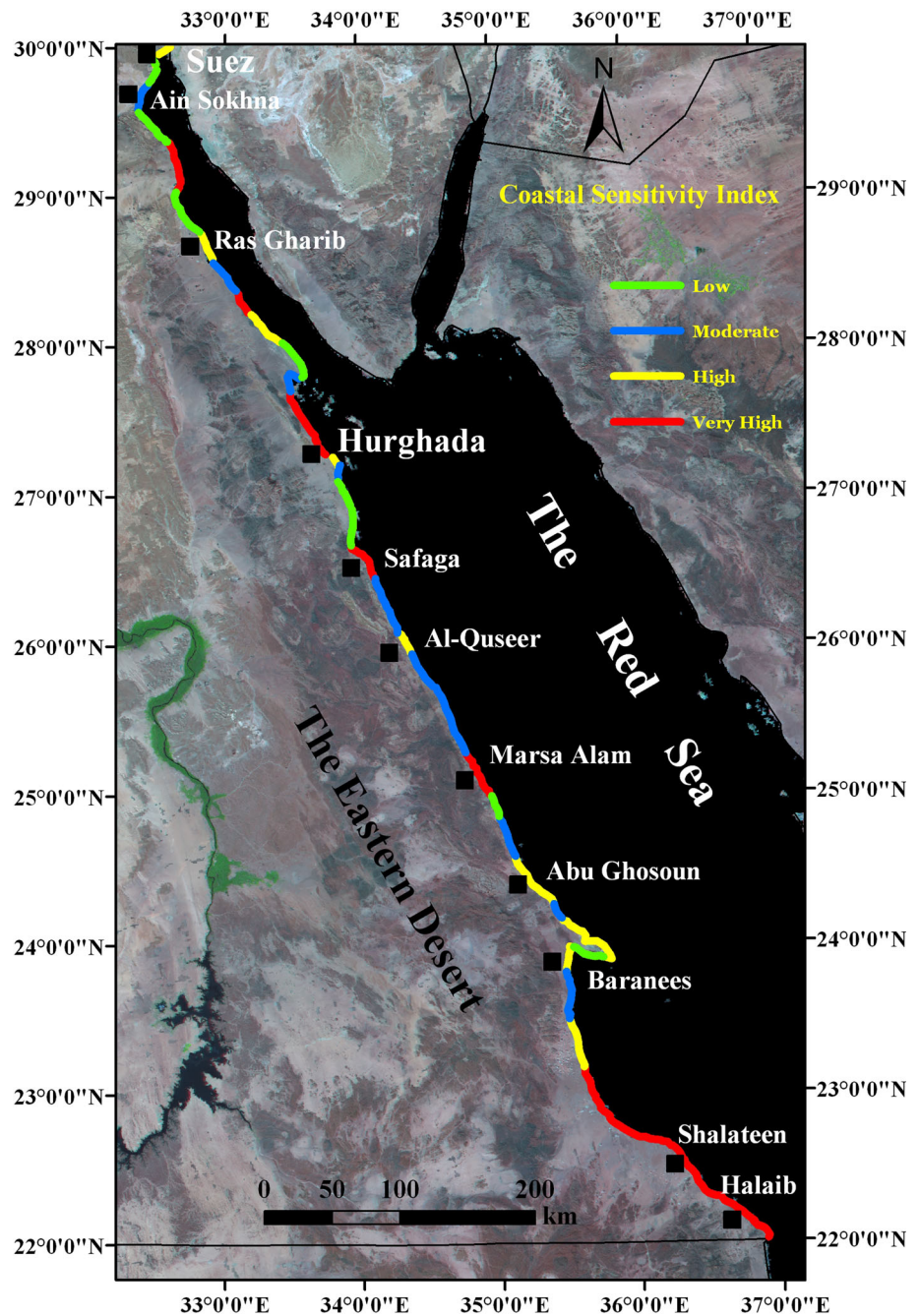
The Red Sea coastal plain varies in width from few meters across the northern parts of the Gulf of Suez to about 35 km in the southern part near Shalateen. In some locations, the coastal plain is nearly absent. Narrow coastal plains (low sensitivity) represent about 19 % along the Gulf of Suez, whereas coastal plain wider than 7.5 km (very high sensitivity) represents 13 % of the coast, particularly at Shalateen. There are about 30 % of the coastal plains ranging in width from 2.5 to 5 km and, hence, the risk is ranked as moderate and they occur between Hurghada and Ras Banas. The rest of the coastal plain (5–7.5 km) account for the remaining 37 % of the coast and is ranked as highly sensitive.

### Shoreline exposure

Shoreline exposure has been applied by Abuodha and Woodroffe (2010) to determine the coastal sensitivity of



**Fig. 5** A map of the Red Sea coast showing the coastal sensitivity levels to climate change



southeast Australian coast to the sea level rise. Wind data of Hurghada reveal that the NW winds prevail for about 54 % of the time and the remaining significant directions are the north (20 %) and the west (14 %). Accordingly, the direction of waves and currents are generally from the northwest. Shoreline exposure to the dominant wave and current directions reveals that the majority of the coastline is ranked as highly exposed for 58 % of the coast, whereas the very high exposed coasts account for 22 %. Moderately exposed shores represent 13 % and sheltered coasts were recorded at only 7 % of the entire coast. The protected shorelines are

generally those which occur in the south-facing lagoons and along the southern fringes of Ras Bans Peninsula.

**Fauna/flora**

Due to its richness in coral reefs and mangrove vegetation, the Red Sea coast includes significant occurrence (38 %) of very high sensitive ecosystems to global warming and sea level rise. Most threaten locations extend between Hurghada and Marsa Alam. Coral reefs exist in parallel lines ranging in width between 50 and 100 m and their density

increases southward until the south of Marsa Alam (Abu Al-Izz 1971). Mangrove forests were recorded from Hurghada southward and they are represented by *Avicennia marina* species (Zahran and Willis 2009). Mangrove forests are confined to shallow water of lagoons and bays and are sensitive to sea level change (IPCC 2001). Highly sensitive coastal strips include the coastal face of dry streams terminating at the Red Sea (26 %). These areas contain important ecosystems, such as littoral salt marshes. Major plant species of these areas are *Phoenix dactylifera*, *Zygophyllum album*, *Tamarix niltica* and *Nitraria retusa* (Zahran and Willis 2009). Moderately threaten coasts comprise consolidated sedimentary shorelines and represent 25 % of the coast. The low vulnerable strips (11 %) include the barren rocky shores of the Gulf of Suez.

### Land use

The coastal vulnerability pertaining to the land use is very high for the coastal cities along the study area (Suez, Ras Gharib, Hurghada, Safaga, Al-Quseer, Marsa Alam, Shalateen and Halaib). These cities cover 30 % of the coast. The region also includes some historic locations since the Coptic and Islamic eras. Hurghada is the capital of the Red Sea Governorate, where most of the government facilities exist. It is an international resort destination for diving and desert tourism. Marsa Alam is also an important diving destination due to the coral reef communities. Population of the region (340,000) are less than 0.5 % of Egypt's population, however, the region is witnessing exponential development activities, particularly in the tourism sector. Highly vulnerable land use includes the main harbors (Suez, Ain Sokhna, Safaga and Abu Ghosoun), which represents 5 % of the coast. Ain Sokhna harbor is a container platform, Safaga harbor is mainly a marine route for transportation with KSA and Abu Ghosoun port is used to export economic ores, such as phosphate. There are two protected areas, Wadi El-Gimal (south of Marsa Alam) and Gebel Elba (south of Shalateen), which account for 7 % of the coast and are considered moderately vulnerable strips. These protected areas contain highly biologic diversity with some important animal species, such as reptiles and amphibians as well as plant species, such as *acacia* spp. Barren and abandoned strips are the dominant across the coast. They approach 58 % of the study area and are ranked as low sensitive to the sea level rise.

### Coastal sensitivity index

The coastal sensitivity index provides a synoptic assessment of the Red Sea coast to climate change as it reflects the net response of the intrinsic behavior of the coast parameters to climate change. The sensitivity classification

indicates that over 365 km (30 %) of the Red Sea coast is under very high coastal sensitivity (Fig. 5), mostly at the inhabited regions (Hurghada, Safaga, Marsa Alam and the southern coast at Shalateen and Halaib). Highly sensitive coastal areas account for 290 km (24 %) and include the coastal sectors at Suez, Ras Gharib, Al-Quseer, and Abu Ghosoun. The intrinsic nature of the coast has increased the susceptibility to sea level rise. Most of these coasts have low resistance to storm waves, flat, wide and are occupied by urban or by coral reef/mangrove communities. Moderately sensitive coasts approach 300 km (25 %) and they mainly comprise the region between Safaga and Marsa Alam. Although this coastal strip is rich in coral reefs, which are sensitive to global warming, their occurrence provides natural protection against storm waves. The least vulnerable locations (245 km) are mostly barren, rocky, narrow, sheltered and/or abandoned shores. They occur mainly along the Gulf of Suez, where the rigorous nature of the rocky shores afford considerable resistance against waves and storms at the time where they are poor in marine organisms that require attachment tools to fix themselves at these rocky shores. Field observations reveal a coincidence with the results obtained from the calculated CSI (Fig. 6). Exposed and wide coastal flats of mangrove ecosystems (at Safaga) have very high CSI (Fig. 6a). The mouth of Wadi El-Gimal (60 km south of Marsa Alam), which is exposed, undulating and rich in palm trees vegetation has high CSI (Fig. 6b). Coastal terraces between Al-Quseer and Marsa Alam, which are narrow, elevated and partially exposed have moderate CSI (Fig. 6c). Coastal resorts constructed on terraces flanked by mountains (15 km south of Marsa Alam) have low CSI (Fig. 6d) and are considered protected from the consequences of climate change.

### Discussion

Egypt faces the Mediterranean Sea from the north and the Red Sea from the east. However, the nature of the response to climate change is different, due to the innate characteristics of each of them. The most pronounced feature of the Mediterranean Sea in Egypt is the occurrence of significant deltaic sediments distributed along nearly 250 km of the entire coast across the Nile Delta. This broad fan is severely prone to inundation by the sea level rise due to the low-resistance nature of the coast and the occurrence of about one-fifth of the delta area below the mean sea level (Hereher 2010). On the other hand, the configuration of the Red Sea coast depicts the tectonic origin, where uplifting associated with the opening of the Red Sea and the splitting of the African plate away from the Arabian plate some 30 million years ago (Wolfenden et al. 2004) is conspicuous. With the exception of a little segment in the southern part,

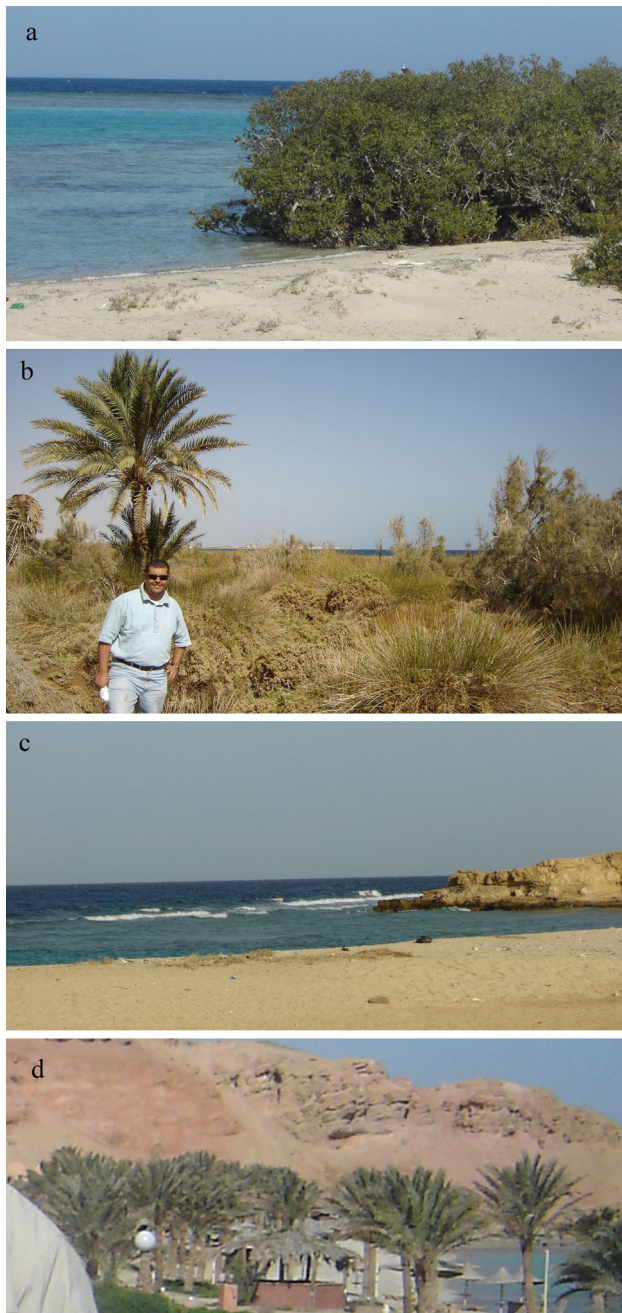


**Fig. 6** Selected locations across the study area to validate the calculated CSI. Letters **a** through **d** represent the net sensitivity levels, which coincide with field observations, as following: **a** is a coastal flat at Safaga coast occupied by Mangrove vegetation, its CSI is very high; **b** is the mouth of Wadi El-Gimal at about 60 km south of Marsa Alam, its CSI is high; **c** a coastal terrace between Al-Quseer and Marsa Alam, its CSI is moderate; and **d** is a coastal resort at 15 km south of Marsa Alam flanked by a mountainous range, its CSI is low

the Red Sea coast is generally composed of raised terraces reflecting the fluctuation of the sea level as a result of plate tectonic adjustments.

The Red Sea coast is under the influence of climate change in two ways: (1) by the sea level rise and (2) by the

increased seawater temperature and atmospheric  $\text{CO}_2$  concentrations. The sea level rise could be either slowly by melting of ice sheets in the poles or accidental by any violent tidal tsunami waves. Tsunami events are not uncommon phenomena in this active tectonic region, where paleo-tsunami deposits were recorded along the Gulf of Suez as a result of rifting activities (Salem 2009). The rocky and cliffy nature of the coast, particularly along the Gulf of Suez combined with the high seismic activity along the fault systems in the region (Arnous et al. 2011; Finkl et al. 2012) possess a potential hazard for land sliding and consequent high tidal waves created by the mass wasting of heavy rocky blocks into the sea. Sea level rise should overwhelm coastal flats, estuaries and bays over which most of coastal cities, harbors and resort villages occur (Fig. 5). The most vulnerable location to the sea level rise is recorded for the bay extending between Ras Banas and Shalateen at the south ( $\text{CSI} = 22.63$ ). DEM data reveal that the slow rise in the sea level by 1 m should overwhelm  $106 \text{ km}^2$ , whereas any sudden rise of the water level by tsunami waves of 5 m height would inundate  $724 \text{ km}^2$  of the coast. Biological resources, such as mangroves, which occur mainly at Safaga region are within the sensitive regions to sea level change as they are contingent to the intertidal zone. The raised terraces, which are mostly uninhabited are generally far from inundation by the slow sea level rise. However, they are not protected if any sudden tsunami waves occur.

The increased water temperature caused by the global warming has a fatal impact upon coral reef ecosystems by losing algal symbiosis with coral organisms (McWilliams et al. 2005). Recent studies have shown slowing of coral reef growth in the Red Sea due to global warming (Cantin et al. 2010). The Hurghada–Marsa Alam coastal strip that extends to 270 km is the most susceptible to changing seawater temperature, where coral reefs are prominent across the coast and they constitute the glorious marine scenery of the region. Coral reefs along the Red Sea coast are considered sub-surface wave breakers that protect the shore from erosion (Frihy et al. 2004). Seawater acidification is a direct impact of the increased  $\text{CO}_2$  concentrations in the atmosphere caused by anthropogenic activities (Coles and Brown 2003). With increased atmospheric  $\text{CO}_2$  concentrations, the water pH should lower and calcification rates of coral calcic skeletons would be impaired (Collingham and Huntley 2000). Therefore, reducing the incidence of these ecosystems could trigger wave action along the coast. Coral reefs are also susceptible to marine pollution caused by human activities. There is a wide range of pollution sources ranging from oil spills to dumping of treated wastewater from resort villages into the sea. The Red Sea is one of the fast growing offshore oil production areas and connection routes for oil in the world. Oil

pollution was reported in Ras Mohammed at the entrance of the Gulf of Suez (Abdel-Kader et al. 1998). Construction of new coastal resorts evolves sediments and wastewater that could potentially disrupt coral reef ecosystems.

A key issue for the coastal zone management is to identify how and where emergency and repatriation plans should be adopted across the coast. The high sensitivity of the study area to climate change, which approach 55 % of the 1200 km long coast, entails the construction of an environmental emergency center to implement warning systems, to update fluctuations of the sea level and water temperature, to provide guide and instructions for local people, and to promote public awareness about deportation from impacted sites particularly in case of tsunami events. Such a center should be equipped with suitable tools and facilities for oceanographic studies and seismic monitoring of the region. Coastal protection measures should also be implemented across the sandy beaches of the region.

## Conclusions

Geologic evolution of the Red Sea has developed a straight and mainly rocky coastal plain. The absence of significant ephemeral fluvial systems and the occurrence in the subtropical region helped for the incidence of significant assemblages of coral reef ecosystems. In addition to their ecological importance, coral reefs are good natural protectors for the coastline from erosion. However, coral reefs are delicate marine ecosystems, which are subtle to climate change. Their deterioration not only exacerbates marine biodiversity but may reduce coastal resistance to storm waves. Coastal geomorphology (landforms) and slope are the most pronounced factors that determine the severely impacted coastal areas along the Red Sea. Sandy flat beaches in Shalateen region are the most sensitive to the sea level rise, whereas the rocky and mountainous shores along the Gulf of Suez exhibit the least sensitivity to sea level rise. The coastal sensitivity map produced from the present study could be used as a guide for coastal planners and conservation managers as well as official agencies in order to get a synoptic and comprehensive prospective for coastal protection. The present study recommends constructing an environmental emergency center devoted to coastal research and for public awareness of the impacts of the sea level rise.

**Acknowledgments** The author deeply acknowledges and thanks the reviewer(s) of the MS for the valuable comments and revisions.

## References

Abdel-Kader A, El-Raey M, Nasr M, El-Gamily H (1998) Environmental sensitivity analysis of potential oil spill for Ras Mohammed coastal zone, Egypt. *J Coastal Res* 14:502–510

- Abu Al-Izz M (1971) Landforms of Egypt. The American University in Cairo Press, p 281
- Abuodha P, Woodroffe C (2010) Assessing vulnerability to sea-level rise using a coastal sensitivity index: a case study from southeast Australia. *J Coast Conserv* 14:189–205
- Al-shalabi M, Billa L, Pradhan B, Mansor S, Al-Sharif AA (2013) Modelling urban growth evolution and land-use changes using GIS based cellular automata and SLEUTH models: the case of Sana'a metropolitan city, Yemen. *Environ Earth Sci* 70(1):425–437
- Arnott RD (2010) Introduction to coastal processes and geomorphology. Cambridge University Press, NY, p 442
- Arnous M, Aboulela H, Green D (2011) Geo-environmental hazards assessment of the north western Gulf of Suez, Egypt. *J Coast Conserv* 15:37–50
- Bathrellos GD, Papanastassiou KG, Skilodimou HD, Papanastassiou D, Chousianitis KG (2012) Potential suitability for urban planning and industry development using natural hazard maps and geological–geomorphological parameters. *Environ Earth Sci* 66:537–548
- Bathrellos GD, Papanastassiou KG, Skilodimou HD, Skianis GA, Chousianitis KG (2013) Assessment of rural community and agricultural development using geomorphological–geological factors and GIS in the Trikala prefecture (Central Greece). *Stoch Environ Res Risk Assess* 27(2):573–588
- Boruff BJ, Emrich C, Cutter SL (2005) Erosion hazard vulnerability of US coastal counties. *J Coastal Res* 21:932–943
- Cantin NE, Cohen AL, Karnauskas KB, Tarrant AM, McCorkle DC (2010) Ocean warming slows coral growth in the central Red Sea. *Science* 329(5989):322–325
- Caragnano A, Colombo F, Rodondi G, Basso D (2009) 3-D distribution of nongeniculate corallinales: a case study from a reef crest of South Sinai (Red Sea, Egypt). *Coral Reefs* 28(4):881–891
- Chaaban F, Darwishe H, Louche B, Queney YB, Masson E, El Khattabi J, Carlier E (2012) Geographical information system approach for environmental management in coastal area (Hardelot-Plage, France). *Environ Earth Sci* 65:183–193
- Churchill J, Lentz S, Farrar J, Abualnaja Y (2014) Properties of Red Sea coastal currents. *Continental Shelf Res* 78:51–61
- Coles SL, Brown BE (2003) Coral bleaching: capacity for acclimatization and adaptation. *Adv Mar Biol* 46:183–223
- Collingham YC, Huntley B (2000) Impacts of habitat fragmentation and patch size upon migration rates. *Ecol Appl* 10:131–144
- Davis R (1996) Coasts. Prentice Hall, Upper Saddle
- Doukakis E (2005) Coastal vulnerability and risk parameters. *European Water* 11(12):3–7
- Duriyapong F, Nakhapakorn K (2011) Coastal vulnerability assessment: a case study of Samut Sakhon coastal zone. *Songklanakarin J Sci Technol* 33:469–476
- El Moursi M, Hoang C, El Fayoumy I, Hegab O, Faure H (1994) Pleistocene evolution of the Red Sea coastal plain, Egypt: evidence from uranium-series dating of emerged reef terraces. *Quat Sci Rev* 13:345–359
- Finkl C (2004) Coastal classification: systematic approaches to consider in the development of a comprehensive scheme. *J Coast Res* 20:166–213
- Finkl C, Pelinovsky E, Cathcar R (2012) A review of potential tsunami impacts to the Suez Canal. *J Coast Res* 28:745–759
- Frihy O, El Ganaini M, El Sayed W, Iskander M (2004) The role of fringing coral reef in beach protection of Hurghada, Gulf of Suez, Red Sea of Egypt. *Ecol Eng* 22:17–25
- Frihy O, Hassan A, El Sayed W, Iskandera M, Sherif M (2006) A review of methods for constructing coastal recreational facilities in Egypt (Red Sea). *Ecol Eng* 27:1–12

- Hammar-Klose ES, Pendleton EA, Thieler ER, Williams SJ (2003) Coastal vulnerability assessment of Cape Cod national seashore (CACO) to sea-level rise, US Geological Survey, Open file Report 02–233
- Hereher M (2010) Vulnerability of the Nile Delta to sea level rise: an assessment using remote sensing. *Geomat Nat Hazards Risk* 1:315–321
- Hereher M (2014) Assessment of South Sinai Coastal vulnerability to climate change. *J Coast Res*. doi:10.2112/JCOASTRES-D-14-00018.1
- Hereher M (2015) Coastal vulnerability assessment for Egypt's Mediterranean coast. *Geomat Nat Hazards Risk* 6(4):342–355
- Hereher M, El-Ezaby K (2012) Soil and water quality assessment along the Red Sea coast, Egypt. *Int J Environ Stud* 69(1):65–77
- Hughes TP, Baird AH, Bellwood DR, Card M, Connolly SR, Folke C, Hoegh Grosberg R, Guldberg O, Jackson JC, Kleypas J, Lough JM, Marshall P, Nystrom M, Palumbi SR, Pandolfi JM, Rosen B, Roughgarden J (2003) Climate change, human impacts, and the resilience of coral reefs. *Science* 301:929–933
- IPCC (Intergovernmental Panel on Climate Change) (2001) Climate change 2001. The scientific basis. Contribution of Working Group I to the Third Assessment Report of the Intergovernmental Panel on Climate Change. In: Houghton JT, Ding Y, Griggs DJ, Noguer, M, van der Linden PJ, Dai X, Maskell K, Johnson CA (eds) Cambridge University Press, Cambridge, New York, p 881
- Johnston A, Slovinsky P, Yates K (2014) Assessing the vulnerability of coastal infrastructure to sea level rise using multi-criteria analysis in Scarborough, Maine (USA). *Ocean Coast Manag* 95:176–188
- Kleypas JA, Buddemeier RW, Archer D, Gattuso JP, Langdon C, Opdyke BN (1999) Geochemical consequences of increased atmospheric carbon dioxide on coral reefs. *Science* 284(5411):118–120
- Kumar TS, Mahendra RS, Nayak S, Radhakrishnan K, Sahu KC (2010) Coastal vulnerability assessment for Orissa State, East Coast of India. *J Coast Res* 26(3):523–534
- Kunte PD, Jauhari N, Mehrotra U, Kotha M, Hursthouse AS, Gagnon AS (2014) Multi-hazards coastal vulnerability assessment of Goa, India using geospatial techniques. *Ocean Coast Manag* 95:264–281
- McWilliams JP, Cote IM, Gill JA, Sutherland WJ, Watkinson A (2005) Accelerating impacts of temperature-induced coral bleaching in the Caribbean. *Ecol* 86(8):2055–2060
- Meehl GA, Washington WM, Collins WD, Arblaster JM, Hu A, Buja LE, Strand WG, Ten H (2005) How much more global warming and sea level rise. *Science* 307:1769–1772
- Nicholls RJ (2002) Analysis of global impacts of sea-level rise: a case study of flooding. *Phys Chem Earth* 27(32–34):1455–1466
- Ozyurt G, Ergin A (2010) Improving coastal vulnerability assessments to sea-level rise: a new indicator-based methodology for decision makers. *J Coast Res* 26(2):265–273
- Papadopoulou-Vrynioti K, Bathrellos GD, Skilodimou HD, Kaviris G, Makropoulos K (2013) Karst collapse susceptibility mapping considering peak ground acceleration in a rapidly growing urban area. *Eng Geol* 158:77–88
- Pendleton EA, Thieler ER and Williams SJ (2004) Coastal vulnerability assessment of Cap Hettaras national seashore (CAHA) to sea level rise. US Geological Survey Open-File Report 2004–1064
- Pendleton EA, Thieler ER and Williams SJ (2005) Coastal vulnerability assessment of Golden Gate national recreation area to sea-level rise. US Geological Survey Open-File Report 2005–1058, p 27
- Plaziat J, Baltzer F, Choukri A, Conchon O, Freydet F (1995) Quaternary changes in the Egyptian shoreline of the northwestern Red Sea and Gulf of Suez. *Quat Int* 29(30):11–22
- Rao KN, Subraeu P, Rao T, Malini B, Ratheesh R, Bhatta-charya S, Rajawat A (2008) Sea-level rise and coastal vulnerability: an assessment of Andhra Pradesh coast, India through remote sensing and GIS. *J Coast Conserv* 12(4):195–207
- Reefbase (2013) Reefbase—a global information system for coral reefs. <http://www.reefbase.org>
- Saad A (2010) Wave and wind conditions in the Red Sea—a numerical study using a third generation wave model. M.Sc. Thesis in Physical Oceanography. Geophysical Institute, University of Bergen, Norway, p 88
- Said R (1962) The geology of Egypt. Elsevier, New York, p 377
- Salem S (2009) Paleo-tsunami deposits on the Red Sea beach, Egypt. *Arab J Geosci* 2:185–197
- Skilodimou HD, Stefouli M, Bathrellos GD (2002) Spatio-temporal analysis of the coastline of Faliro Bay, Attica, Greece. *Estud Geol Madrid* 58(3–4):83–89
- Small C, Nicholls RJ (2003) A global analysis of human settlement in coastal zones. *J Coast Res* 19(3):584–599
- Thieler ER, Hammar-Klose ES (1999) National assessment of coastal vulnerability to sea-level rise: preliminary results for the US Atlantic Coast US Geological Survey, Open-File Report 99–593, 1 sheet
- Uddameri V, Singaraju S, Hernandez EA (2014) Impacts of sea-level rise and urbanization on groundwater availability and sustainability of coastal communities in semi-arid South Texas. *Environ Earth Sci* 71(6):2503–2515
- Williams S (2013) Sea-level rise implications for coastal regions. *J Coastal Res* 63:184–196
- Wolfenden E, Ebinger C, Yirgu G, Deino A, Ayele D (2004) Evolution of the northern main Ethiopian Rift: birth of a triple junction. *Earth Planet Sci Lett* 224:213–228
- Youssef AM, Maerz NH (2013) Overview of some geological hazards in the Saudi Arabia. *Environ Earth Sci* 70(7):3115–3130
- Zahrán M, Willis A (2009) The vegetation of Egypt. Springer Science Bus Media, Berlin, p 437